The Rydberg states of H_2O

M. S. Child

Email alerting service	Receive free email alerts when new articles cite this article - sign up in the box at the top right-hand corner of the article or click **here**

The Rydberg states of H_2O

By M. S. Child

*Physical and Theoretical Chemistry Laboratory, University of Oxford,
South Parks Road, Oxford OX1 3QZ, UK*

Empirical quantum defect functions are fit to the vibrational origins of the known
rotationally resolved bands of H_2O and D_2O, including new analyses for bands in
the region of the 3d (100) clusters. Consolidation of the H_2O and D_2O data allows
an extrapolation of the 3p (0 v_2 0) $^1B_2$ and 3p (1 v_2 0) $^1B_2$ linear state bending
progressions as a means of rationalizing known perturbations and predissociations
in the 3d clusters and of estimating their influence on the higher nd series. A new
vibronic mechanism for autoionization from the 3d b_1 $^1B_1$ linear state vibrational
progression is found to be in excellent agreement with the observed autoionization
rate.

1. Introduction

The Rydberg spectrum of H_2O is one of the best characterized of any polyatomic
species, but severe complications arise from the occurrence of strong Renner–Teller
coupling between the bent $\tilde{X}$ $^2B_1$ and linear $\tilde{A}$ $^2A_1$ states of the H_2O^+ positive ion.
In the first place, every $\ell\lambda$ Rydberg series (where λ denotes symmetry under C_{2v})
consists of an associated bent/linear pair converging on the coupled positive ion
states. Secondly linear states of lower $(n\ell\lambda \leftarrow 3a_1)$ states derived from $\tilde{A}$ $^2A_1$ of the
ion can have strong configuration interactions with higher lying bent $(n'\ell'\lambda' \leftarrow 1b_1)$
states that converge on $\tilde{X}$ $^2B_1$ of H_2O^+; evidence of such interactions between $\tilde{B}$ $^1B_1$
$(3sa_1 \leftarrow 1b_1)$ and $\tilde{D}$ $^1B_1$ $(3pb_1 \leftarrow 3a_1)$ and between $\tilde{E}'$ $^1B_2$ $(3da_2 \leftarrow 1b_1)$ and the
linear $^1B_2$ $(3pb_2 \leftarrow 3a_1)$ state is clearly seen in the calculations of Theodorakopoulos
et al. (1984) and Hirst & Child (1992) and a strong resulting perturbation to the
3d (000) cluster from the latter has been observed experimentally (Gilbert *et al.*
1991). Finally any spectroscopic analysis is complicated by the dissociative character
of at least the $\tilde{A}$ $^1B_1$ $(3sa_1 \leftarrow 1b_1)$ and the unobserved $^1A_2$ $(3pb_2 \leftarrow 1b_1)$ states,
which seems to be carried to the rest of the spectrum by some sequence of Renner–
Teller and configuration interactions. For example the $\tilde{B}$ $^1A_1$ $(3sa_1 \leftarrow 3a_1)$ state
is strongly predissociated by Renner–Teller coupling to $\tilde{A}$ $^1B_1$ (Dixon 1985) and a
similar Renner–Teller mechanism via $^1A_2$ $(3pb_2 \leftarrow 1b_1)$ is undoubtedly responsible
for the absence of $K' \neq 0$ branches in the linear $^1B_2$ $(3pb_2 \leftarrow 3a_1)$ state spectrum
(Abramson *et al.* 1990). The absence of rotational structure in the $\tilde{D}$ $^1A_1 \leftarrow \tilde{A}$ $^1A_1$
spectrum (Bell 1965) is confidently attributed to configuration interaction with the
$\tilde{B}$ $^1A_1$ state and there is also evidence of rotationally selective predissociation in
many of the rotationally analysed bands (Ashfold *et al.* 1984b; Gilbert *et al.* 1991)
although the precise mechanism remains to be understood. Detailed analysis has been
largely restricted to low-lying bands but the pervasive character of the predissociation

is suggested by excitation of OH $\tilde{A} \to \tilde{X}$ emission even above the ionization limit (Dutuit *et al.* 1985)

The object of this paper is to provide a quantum defect synthesis of all the known rotationally analysed bands of H_2O and D_2O in order to aid the accurate prediction of unobserved term values and the identification of spectral perturbations between the bent nd series and the linear $3p\ {}^1B_2$ state. Secondly a new vibronic autoionization mechanism is suggested to account for photoionization from the $3db_1\ {}^1B_1$ linear state, which leads to an ionization rate in good agreement with the estimated autoionization contribution to the linewidths observed by Dehmer & Holland (1991).

2. Theoretical model

The theoretical model complements the *ab initio* work of Petsalakis *et al.* (1995) and Theodorakopoulos *et al.* (1996) which yields an excellent global synthesis of interactions between different members of successive Rydberg series. The potential surfaces for individual high lying Rydberg states are not, however, sufficiently accurate to allow the prediction of vibrational term values within say $10\ \mathrm{cm}^{-1}$.

The present approach is to recognise that the $J = 0$ term values for any vibronic state are unaffected by Coriolis complications (or rotational channel interactions in the language of Greene & Jungen (1985)). Hence in the absence of vibrational perturbations (which we seek to identify) the required vibrational energies may be calculated by the following quantum defect representation of the Born–Oppenheimer potential surface

$$V_{in\ell\lambda}(\boldsymbol{Q}) = V_i^+(\boldsymbol{Q}) - \frac{Ry}{[n - \mu_{\ell\lambda}(\boldsymbol{Q})]^2} + I_e'. \tag{2.1}$$

where $\boldsymbol{Q}$ denotes the vibrational coordinates.

Accurate positive potential energy surfaces $V_i^+(\boldsymbol{Q})$ for the relevant core states $i = \tilde{X}\ {}^2B_1$ and $\tilde{A}\ {}^2A_1$ are provided by Brommer *et al.* (1993). The quantum defect functions $\mu_{\ell\lambda}(\boldsymbol{Q})$ for different Rydberg series were taken in the forms

$$\mu(\boldsymbol{Q}) = c_0 + c_1/\nu^2(\boldsymbol{Q}) + c_2 \cos\theta + c_3 \cos^2\theta + c_4(\bar{R} - R_0)^2, \tag{2.2}$$

where $\nu(\boldsymbol{Q}) = n - \mu(\boldsymbol{Q})$, θ is the bond angle and $\bar{R}$ is the mean bond length. The absence of spectroscopic data on the antisymmetric stretching mode precludes the inclusion of terms in R_1–R_2 in equation (2.2).

It is convenient for present purposes to measure the ion potential surfaces $V_i^+(\boldsymbol{Q})$ from the minimum of the $\tilde{X}\ {}^2B_1$ state and to employ different 'upper-state equilibrium' ionization potentials I_e' for H_2O and D_2O, which are taken as the energy from the (000) level of the relevant isotopomer to V_e^+ for $\tilde{X}\ {}^2B_1$ of H_2O^+. The calculated vibrational energies then correspond to absorption frequencies from $\tilde{X}$ (000). Given the ionization energies of $101\,766\ \mathrm{cm}^{-1}$ and $101\,916\ \mathrm{cm}^{-1}$ for H_2O and D_2O respectively (Tonkyn *et al.* 1991) and the corresponding calculated H_2O^+ zero point energies $4068\ \mathrm{cm}^{-1}$ and $2978\ \mathrm{cm}^{-1}$ from Weiss *et al.* (1989), the relevant values are $I_e' = 97\,698\ \mathrm{cm}^{-1}$ and $98\,938\ \mathrm{cm}^{-1}$ for H_2O and D_2O, respectively.

The vibrational calculations reported below were derived from the Hamiltonian of Carter *et al.* (1983) by diagonalization in a three mode non-degenerate harmonic oscillator basis for the bent states; degenerate harmonic oscillator functions were employed for bending motions of the linear states. Derivative terms in the kinetic energy were evaluated by use of the harmonic oscillator recurrence relations and potential-like matrix elements were calculated by quadrature. Non-orthogonality between the

basis functions for the relevant bending volume element $\sin\theta\,\mathrm{d}\theta$ (Carter *et al.* 1983) was properly taken into account. Test calculations for H_2O^+ gave agreement with Brommer *et al.* (1993) to within $2\ \mathrm{cm}^{-1}$ for the fundamentals, rising to $10\ \mathrm{cm}^{-1}$ for bending levels with vibrational energies of $15\,000\ \mathrm{cm}^{-1}$.

Autoionization contributions to the linewidth, Γ, were obtained by a perturbative analysis of the coupled channel equations between one bound and one open channel (Greene & Jungen 1985).

$$\det\begin{pmatrix} K_{cc} + \tan\pi\nu(E) & K_{co} \\ K_{oc} & K_{oo} - \tan\pi\tau(E) \end{pmatrix} = 0, \tag{2.3}$$

where

$$\nu(E) = [Ry\,/(E_{v+} - E)]^{1/2}, \tag{2.4}$$

E_{v+} is the series limit of the bound channel and $\tau(E)$ is an eigenphase for the open channel, which follows the Breit–Wigner form

$$\tau(E) = \tau^\circ(E) + \pi^{-1}\arctan[\tfrac{1}{2}\Gamma(E_0 - E)], \tag{2.5}$$

on passing through a resonance at E_0. It may be verified by expanding $\nu(E)$ as

$$\nu(E) = \nu(E_0) + \nu'(E_0)(E - E_0), \tag{2.6}$$

with $\nu_0 = \nu(E_0)$ given by

$$K_{cc} + \tan\pi\nu(E_0) = 0, \tag{2.7}$$

that

$$\Gamma \simeq (4\,Ry\,/\pi)\cos^2\pi\nu_0 K_{oc}^2/\nu_0^3. \tag{2.8}$$

The K matrix elements relevant to interactions between different electronic channels are crudely estimated as a product of the appropriate vibrational overlap $S_{vv'}$ and an electronic K matrix element. The latter is estimated by the requirement that the roots of the bound–bound equivalent of equation (2.3), namely

$$\det\begin{pmatrix} K_{11} + \tan\pi\nu_1(E) & K_{12} \\ K_{21} & K_{22} + \tan\pi\nu_2(E) \end{pmatrix} = 0, \tag{2.9}$$

should reproduce a known or assumed electronic perturbation ΔE_{el}. Following Hirst & Child (1992) the perturbed electronic energies are given by the roots of

$$[E - E_1(\boldsymbol{Q})][E - E_2(\boldsymbol{Q})] = \boldsymbol{V}_{12}^2(\boldsymbol{Q}), \tag{2.10}$$

where

$$V_{12}(\boldsymbol{Q}) = 2(Ry\,/\pi)[\nu_1(E)\nu_2(E)]^{-3/2}\cos\pi\nu_1\cos\pi\nu_2 K_{12}(\boldsymbol{Q}). \tag{2.11}$$

The combined use of equations (2.8) and (2.11) is illustrated in §5 by application to autoionization from the linear $n\mathrm{d}\ ^1B_1$ states. Broadly speaking the electronic K matrix element K_{12} is deduced from an implied electronic energy splitting for $n = 3$, and then converted to a vibrational channel coupling K matrix element K_{oc} by multiplication by the relevant vibrational overlap integral, on the assumption that V_{12} and K_{12} are independent of $\boldsymbol{Q}$.

3. Bent states of H₂O and D₂O

The purpose of the present vibrational synthesis is to identify possible vibrational perturbations and to aid the prediction and analysis of hitherto unanalysed bands by

Table 1. *Empirical quantum defect coefficients defined by equation (2.2)*

channel	c_0	c_1	c_2	c_3	c_4
bent states					
$\tilde{C}$ np $^1B_1$	0.681 81	0.2167	0.000	−0.006	0.097
$\tilde{D}'$ ns $^1B_1$	1.485 64	0.0000	0.181	0.368	0.740
$\tilde{D}''$ nd $^1A_2$	0.388 00	−0.1079	0.188	0.376	−1.500
$\tilde{E}$ nd $^1B_1$	0.152 85	−0.2794	0.000	0.000	0.250
$\tilde{E}'$ nd $^1B_2$	0.055 00	0.1810	0.000	0.000	0.070
$\tilde{F}$ nd $^1B_1$	0.003 24	−0.1685	0.000	0.000	0.085
$\tilde{F}$ nd $^1A_1$	0.019 56	−0.2848	0.000	0.000	−0.050
linear states					
3p $^1B_2$	1.042 74	0.0000	0.000	−0.075	1.000
3d $^1A_1$	0.013 72	−0.042 45	0.050	0.000	0.000

testing for consistency between the vibrational band origins of both H_2O and D_2O. To do this it is necessary to correct for the fact that conventional band origins for states with $\ell \neq 0$ include a purely rotational term $A\ell_a^2 + B\ell_b^2 + C\ell_c^2$, which must be subtracted for a proper comparison. The origins quoted in table 2 are therefore equivalent to the quantities denoted X by Gilbert *et al.* (1991), rather than conventional origins.

Results given in table 2 were fit to experimental data for the 3p and 4p $^1B_1$, the 4s $^1B_1$ and 3d and 6d clusters. The relevant quantum defect coefficients for use in equation (2.2) which are listed in table 1 were fit in the few cases of ambiguity to the levels marked by an asterisk in table 2. The quality of the overall fit is remarkable, bearing in mind that the vibrational fundamentals for a given state of for example H_2O also fix the relative zero-point energies of the isotopomers as well as the vibrational energies of D_2O. The data are presented in terms of the absolute energies of the (000) level for each state, while quantities in parenthesis give excitation energies from this value in order to indicate the magnitudes of discrepancies from the ν_1 and ν_2 fundamentals of H_2O^+ and D_2O^+. Thus it is evident for example that the excellent fit for the $\tilde{C}$ $^1B_1$ states is achieved despite a substantial reduction in ν_1 from 3213 cm^{-1} in H_2O^+ to 3171 cm^{-1}. Comments on the individual entries are given below.

(*a*) *3p and 4p $\tilde{C}$ $^1B_1$ states*

The excellent quality of the fit suggests a reassignment of the H_2O absorption band origin at 86 849 cm^{-1} (Ashfold *et al.* 1984*b*, corrected to 86 806 cm^{-1} in the table) to the 3p $\tilde{C}$ (100) $^1B_1$ state rather than the $\tilde{D}'$ (200) 4s $^1B_1$ state. The only anomaly is then the 3p $\tilde{C}$ (200) level of D_2O which is perturbed by 23 cm^{-1} from its calculated value. It is difficult to suggest an alternative assignment or a plausible perturbing state of the appropriate symmetry.

(*b*) *4s $\tilde{D}'$ $^1B_1$ state*

Consistency between the observed and calculated vibrational levels of H_2O together with the (000) and (010) levels of D_2O argues in favour of the chosen fit, which assumes very substantial changes in ν_1 and ν_2 from their positive ion values.

The levels assigned to (100) and (110) of D_2O are, however, markedly out of line with their calculated values, due possibly to perturbations by high vibrational levels of the $\tilde{C}\ ^1B_1$ state.

(c) 3d–6d clusters

Data on the 3d $\tilde{D}''\ ^1A_2$ state, which is optically inaccessible in absorption, come from the multiphoton studies of Ashfold *et al.* (1984*a*, *b*). Analysis of the room temperature 3d clusters (Gilbert *et al.* 1991, and Appendix A) is probably more reliable for D_2O than for H_2O because Coriolis coupling is weaker and there is less evidence of perturbations; in cases of ambiguity the preferred fit was therefore to the D_2O data. Term values for the 6d (000) clusters and 6d (100) of H_2O were deduced from the quantum defects employed by Vrakking *et al.* (1993); those for 6d (100) of D_2O were inferred from the photoionization spectrum of Page *et al.* (1988), as analysed by Child & Jungen (1990).

Since the available data are limited to (000) and (100) levels, coefficients of the terms in $\cos\theta$ in equation (2.2) were set to zero. Hence the discrepancies between the observed and calculated H_2O and D_2O zero point levels for the 3d $\tilde{E}$ and 3d $\tilde{E}'$ states could imply correction terms to the ion potential $V^+(\boldsymbol{Q})$ for the bending motion. Analysis of very weak H_2O bands between $90\,150\ \mathrm{cm}^{-1}$ and $91\,500\ \mathrm{cm}^{-1}$ which are tentatively assigned to the 3d (010) cluster by Mayhew (1984) would clarify the picture. Entries in table 2 for the 4d and 5d (000) and (100) clusters are included to aid subsequent analysis of these bands.

The $^1A_2$ components of the nd clusters present a special challenge because only a few 3d members have been directly observed (Ashfold *et al.* 1984). Information on the 6d members is, however, available from their Coriolis effects on the $\tilde{E}$ and $\tilde{E}'$ components. One sees by comparison with the positive ion frequencies that the $^1A_2$ surfaces appear to be strongly distorted from that of the positive ion. It is also noticeable that the calculated 3d (000) level for D_2O lies almost $160\ \mathrm{cm}^{-1}$ above the reported value. Given the overall remarkable consistency of the quantum defect construction it is hard to understand this huge discrepancy, because Ashfold *et al.* (1984*a*) report a convincing simulation of the relevant band.

4. The linear 3p $^1B_2$ state

Knowledge of the linear 3p $^1B_2$ state is of considerable importance for future analysis of the nd $\leftarrow 1b_1$ clusters, in view of its known strong interaction with the 3d (000) $\tilde{E}\ ^1B_2$ state (Gilbert *et al.* 1991) and the fact that its $K' \neq 0$ rotational levels are strongly predissociated (Abramson *et al.* 1990). Strong predissociation in the 3d (100) $\tilde{E}'\ ^1B_2$ bands of both H_2O and D_2O reported in Appendix A is probably due to these two factors. Similar effects are also expected for higher nd states because the linear 3p $^1B_2$ bending potential appears to cut through all the bent nd $\tilde{E}'\ ^1B_2$ state potentials (Hirst & Child 1992; Theodorakopoulos *et al.* 1996).

The reported vibrational assignments (Abramson *et al.* 1990), which were made by comparison with the photoelectron spectrum of Dixon *et al.* (1976), are here reassigned upwards by two units in v_2, in line with the recommendations of Reuter *et al.* (1991) and Brommer *et al.* (1993), because the carefully determined $\tilde{A}\ ^2A_1$ potential of H_2O^+ from the latter authors was employed as $V^+(\boldsymbol{Q})$ in equation (2.1). Optimization of the quantum defect coefficients in equation (2.2) demonstrated the need for a substantial change in stretching contributions to the zero-point energy

1628   M. S. Child

Table 2. *Bent $\tilde{D}'$ 4s $^1B_1$, $\tilde{C}$ np $^1B_1$ and nd states. Values in parenthesis are measured from the (000) level*

channel	n	v_1	v_2	v_3	H₂O		D₂O	
					G_{obs} (cm^{-1})	G_{calc} (cm^{-1})	G_{obs} (cm^{-1})	G_{calc} (cm^{-1})
$\tilde{C}$ np $^1B_1$	3	0	0	0	[n]80 587[a]	80 585	[n]80 731[a]	80 738
		0	1	0	(1402)[a]	(1401)	(1038)[a]	(1040)
		0	2	0	—	(2756)	(2016)[b]	(2056)
		1	0	0	(3171)[b]	(3169)	(2319)[b]	(2318)
		2	0	0	[o](6227)[b]	(6229)	(4609)[b]	(4586)
	4	0	0	0	91 670[c]	91 671	91 827[c]	91 821
$\tilde{D}'$ ns $^1B_1$	4	0	0	0	84 434[d]	84 434	84 646[c]	84 649
		0	1	0	(1138)[d]	(1138)	(855)[d]	(851)
		1	0	0	(2964)[d]	(2964)	(2166)[d]	(2180)
		1	1	0	—	(4110)	(3072)[d]	(3039)
$\tilde{D}''$ nd $^1A_2$	3	0	0	0	[n]86 178[d]	86 178	[n]86 145[d]	86 304
		0	1	0	(1191)[d]	(1191)	—	(885)
		1	0	0	—	(3556)	—	(2584)
	4	0	0	0	—	93 520	—	93 657
		1	0	0	—	96 872	—	96 100
	5	0	0	0	—	96 682	—	96 824
		1	0	0	—	99 963	—	99 218
	6	0	0	0	98 322[e]	98 322	—	98 467
		1	0	0	101 582[e]	101 573	100 852[f]	100 840
$\tilde{E}$ nd $^1B_1$	3	0	0	0	88 503[g]	88 530	[*]88 686[g]	88 684
		1	0	0	—	(3160)	[*](2312)[c]	(2312)
	4	0	0	0	—	94 416	—	94 567
		1	0	0	—	97 606	—	96 899
	5	0	0	0	—	97 116	—	97 264
		1	0	0	—	100 316	—	99 603
	6	0	0	0	[*]98 565[e]	98 565	—	98 713
		1	0	0	101 785[e]	101 770	101 050[f]	101 055
$\tilde{E}'$ nd $^1B_2$	3	0	0	0	[*]88 928[g]	88 928	89 090[g]	89 077
		1	0	0	[*](3197)[c]	(3197)	—	(2337)
	4	0	0	0	—	94 673	—	94 821
		1	0	0	—	97 878	—	97 163
	5	0	0	0	—	97 266	—	97 413
		1	0	0	—	100 474	—	99 757
	6	0	0	0	[*]98 656[e]	98 656	—	98 805
		1	0	0	101 862[e]	101 867	101 145[f]	101 150

Table 2. *(Cont.)*

channel	n	v_1	v_2	v_3	H₂O		D₂O	
					G_{obs} (cm^{-1})	G_{calc} (cm^{-1})	G_{obs} (cm^{-1})	G_{calc} (cm^{-1})
$\tilde{F}$ nd $^1B_1$	3	0	0	0	89 696[g]	89 694	*89 843[g]	89 843
		1	0	0	(3212)[c]	(3196)	*(92 336)[c]	(2336)
	4	0	0	0	—	94 932	—	95 080
		1	0	0	—	98 137	—	97 422
	5	0	0	0	—	97 384	—	97 531
		1	0	0	—	100 591	—	99 875
	6	0	0	0	98 716[e]	98 721	—	98 868
		1	0	0	101 928[e]	101 930	101 201[f]	101 213
$\tilde{F}$ nd $^1A_1$	3	0	0	0	89 680[g]	89 681	*89 827[g]	89 827
		1	0	0	—	(3220)	*(2352)[c]	(2352)
	4	0	0	0	—	94 906		95 053
		1	0	0	—	98 121		97 402
	5	0	0	0	—	97 365		97 513
		1	0	0	—	100 579		100 575
	6	0	0	0	*98 707[e]	98 709		98 856
		1	0	0	101 922[e]	101 921	101 207[f]	101 203
positive ion		0	1	0	1408[h]	—	1044[i]	—
		1	0	0	3213[j]	—	2342[k]	—
I (cm^{-1})					101 766[l]		101 916[l]	
G^+ (0,00) (cm^{-1})					4068[m]		2978[m]	

[a]Johns 1963. [b]Ashfold *et al.* 1984*b*. [c]Present (see Appendix A). [d]Ashfold *et al.* 1984*a*. [e]Vrakking *et al.* 1993. [f]Child & Jungen 1990. [g]Gilbert *et al.* 1991. [h]Lew 1976. [i]Lew & Groleau 1987. [j]Reutt *et al.* 1986. [k]Liu *et al.* 1987. [l]Tonkyn *et al.* 1991. [m]Weis *et al.* 1989. [n]Corrected for electronic angular momentum term (see text). [o]Reassigned (see text).

in order to reconcile the absolute frequencies of the (0 v_2 0) progressions of H₂O and D₂O. The whole correction is here attributed to the symmetric stretching mode, with a consequent reduction in ν_1 from 3224.6 cm^{-1} in H₂O$^+$ (Brommer *et al.* 1993) to 2554 cm^{-1} in the linear 3p $^1B_2$ state. Theoretical support for a correction of this magnitude comes from the *ab initio* results of Theodorakopoulos *et al.* (1996), but predictions with respect to $(v_1v_2v_3)$ levels with $v_1 \neq 0$ and $v_3 \neq 0$ must be regarded as indicative rather than quantitative.

The results in table 3 are in good agreement with the observed values, for the final three-parameter fit and little improvement was obtained by simultaneous variation of the coefficient c_2. The vibrational diagonalization was, however, too time consuming for least squares optimization. Predictions for higher bending levels are given to aid their future experimental detection. Values are also given for the overlap integrals with the 3d (000) $^1B_2$ state, which are also assumed to be valid for higher members of the series, in order to estimate the magnitude of possible perturbations.

Figure 1 shows the relative disposition of the nd (000) $^1B_2$ and nd (100) $^1B_2$ vibra-

Table 3. *Linear* 3p $^1B_2$ *state. The quantity S is the overlap with the* 3d *(000)* $^1B_2$ *vibrational state*

	H$_2$O				D$_2$O		
ν_2^c	G_{obs} (cm^{-1})	G_{calc} (cm^{-1})	S	ν_2^c	G_{obs} (cm^{-1})	G_{calc} (cm^{-1})	S
3	84 127[a]	84 211	0.138	7	85 991[b]	86 108	0.142
5	85 714[a]	85 711	0.238	9	87 327[a]	87 323	0.206
7	87 380[a]	87 354	0.309	11	88 582[a]	88 595	0.249
9	89 095[b]	89 096	0.322	13		89 908	0.273
11		90 902	0.283	15		91 248	0.267
13		92 741	0.220	17		92 606	0.240
15		94 592	0.156	19		93 975	0.199
17		96 463	0.097			95 356	0.141
19		98 358	0.059			96 766	0.093
21		100 307	0.035				

[a]Abramson *et al.* (1990). [b]Present (see Appendix A). [c]Reassigned by two units from Abramson *et al.* (1990).

tional states of H$_2$O from table 2 and the 3p $(0\ v_2\ 0)$ $^1B_2$ and 3p $(1\ v_2\ 0)$ progressions. Odd members of the bending progressions have non-predissociated $K' = 0$ rotational states, while even members are thought to be predissociated for all K' values. The known perturbation between 3d (000) $^1B_2$ and 3p (090) $^1B_2$ (Gilbert *et al.* 1991) is analysed in Appendix A to yield an interaction term $V_{12} = 145$ cm^{-1}. Other interactions must scale with the vibrational overlap elements S in table 3 and also with $(n - \mu)^{-3/2}$, by the quantum defect arguments in §2. The corresponding interaction between the close lying 4d (000) and 3p (0 15 0) levels is therefore predicted to fall to $V_{12} \simeq 45$ cm^{-1}, which is comparable with the predicted level separation from tables 2 and 3. Other perturbations by the odd v_2 bending states are expected to be quite small in view of the rapid fall off of V_{12} with S and $(n - \mu)^{-3/2}$.

The predictions concerning the location of low-lying members of the linear 3p $^1B_2$ state progressions are also at least partially confirmed by the evidence of rotationally selective predissociation. For example the fact that the perturbed 3d (000) $\tilde{E}'$ $^1B_2$ band of H$_2$O contains only $K' = 0$ and 1 branches (Gilbert *et al.* 1991) is explained on the basis that the perturbing 3p (090) $^1B_2$ is unpredissociated for $K' = 0$ while $K' = 1$ states are forbidden for odd v_2. Similarly, according to the re-analysis reported in Appendix A, the 3d (000) $\tilde{E}'$ band of D$_2$O contains $K' = 0$ and 2 branches but no $K' = 1$ branches because the perturbation is by the even v_2, 3p (0 12 0) state. A similar situation arises for the 3d (100) $\tilde{E}'$ $^1B_2$ level of H$_2$O, which is predicted to be perturbed by 3p (1 10 0) and only $K' = 0$ branches can be clearly identified. Finally the situation with respect to 3d (100) $\tilde{E}'$ of D$_2$O is less clear because this component of the cluster appears only as scattered diffuse lines.

5. Autoionization from the linear nd $^1B_1$ states

Linear state bending progressions between 950 and 860 Å were ascribed to nd $\leftarrow 3a_1$ transitions by Katayama *et al.* (1973) and Ishiguro *et al.* (1978). The lines are
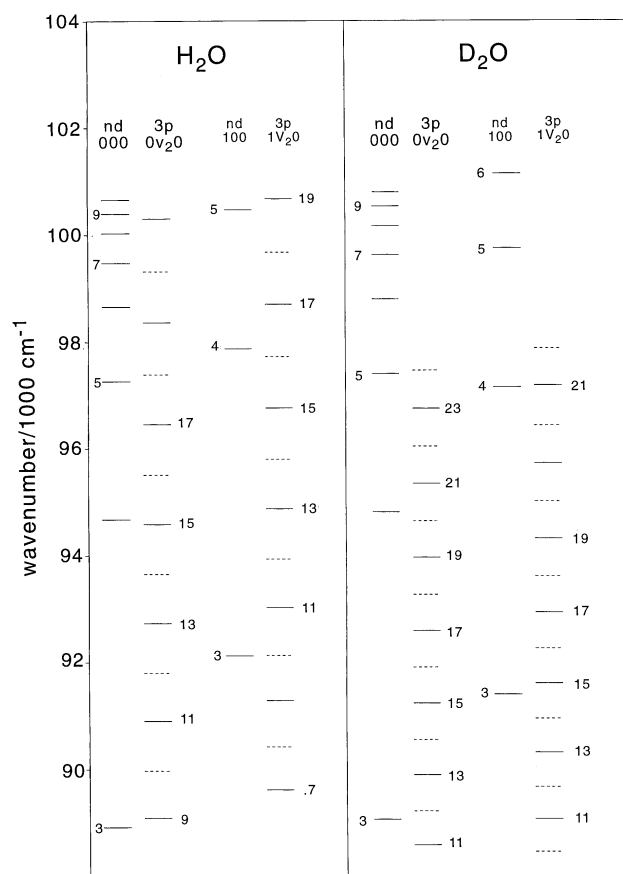
Figure 1. Predicted nd $(v_1\ 0\ 0)$ $\tilde{E}'$ $^1B_2$ and 3p $(v_1\ v_2\ 0)$ $^1B_2$ band origins with $v_1 = 0, 1$ for H_2O and D_2O. Odd v_2 members of the 3p $^1B_2$ are predicted to be unpredissocation for $K' = 0$; even members, which are indicated by dashed lines are predissociated for all K'.

broad, but rotational resolution was achieved by Page *et al.* (1988) and Dehmer & Holland (1991) of whom the latter established a definitive electronic assignment to the linear nd $^1B_1$ series and estimated the rotational linewidths as of order $13\ \mathrm{cm}^{-1}$.

The purpose of the present section is to estimate the contribution to the autoionization linewidth from a new specifically polyatomic vibronic mechanism. The argument is that the upper-most bent nd $(^1A_1,\ ^1B_1)$ pairs and linear nd $(^1A_1,\ ^1B_1)$ pairs derive in linear geometry from a $^2\Pi$ state of H_2O^+ plus an nd δ state of the Rydberg electron. Configuration interaction between the electron and the core therefore results in $^1\Pi$ and $^1\Phi$ terms, split by an energy $2V_{12}$ say. The bent $(nda_1 \leftarrow 1b_1)$ $^1B_1$ and linear $(ndb_1 \leftarrow 3a_1)$ $^1B_1$ states are therefore completely mixed in the linear geometry, but this admixture is progressively quenched as the molecule bends. The rate of autoionization at energies above the bent series limit is here ascribed to the bending sensitivity of these electronic states, of which the linear component is closed and the bent one open to autoionization.

A full Renner–Teller treatment would be required for a definitive treatment, but an order of magnitude estimate of the relation between the configuration interaction term V_{12} and the autoionization rate may be obtained by identifying K_{12} in equation (2.9) as the scattering manifestation of this purely electronic interaction.

Table 4. *Linear nd $^1B_1$ states*

n	v_2^b	G_{obs}^a (cm^{-1})	G_{calc} (cm^{-1})
3	6	102 386	102 386
	8	104 182	104 194
	10	106 080	106 087
	12	108 060	108 042
4	8	109 382	109 375
	10	111 314	111 297
5	8	111 785	111 803
	10	113 702	113 728
	12	115 655	115 713

[a]From Dehmer & Holland (1991) rotational assignments assuming $B' = 8$ cm^{-1}.
[b]Reassigned by units from values of Dehmer & Holland (1991).

The important feature is that K_{12} may be assumed by normal quantum defect arguments to be independent of energy, whereas V_{12} falls off as $[\nu_1(E)\nu_2(E)]^{-3/2}$. Thus K_{12} which will be assumed to be independent of the molecular geometry may be estimated from knowledge of the low nd states (Petsalakis *et al.* 1995, 1997).

The necessary vibrational K matrix element (Ross 1990) appears as $K_{oc} = SK_{12}$ where S is the overlap between the $\tilde{X}$ (000) $^1B_1$ state of H_2O^+ and the 3d (0 v_2 0) $^1B_1$ linear state. It follows on eliminating the K matrix elements between equations (2.8) and (2.11) that

$$\Gamma = [\pi S^2 \nu^3 V_{12}^2 / Ry \cos^2 \pi\nu], \tag{5.1}$$

where V_{12} is the electronic matrix element for the convenient 3d cluster and $\nu = n - \mu$ for the relevant bent 3d state. The above two channel model is clearly oversimplified but it is assumed that the estimate given by equation (5.1) may be summed over the open vibrational channels of the positive ion.

Put in quantitative terms the reasonable values $S = 0.3$ and $\mu \simeq 0$ for each of the two, H_2O^+ $\tilde{X}$ (000) and (010), open channels require an electronic splitting between the two 3dδ $^1B_1$ terms of $2V_{12} \simeq 190$ cm^{-1} in order to account for the autoionization component of the 3d (080) linewidths of 13 cm^{-1}, 80% of which is attributed by Dehmer & Holland (1991) to predissociation on the evidence of Katayama *et al.* (1973).

As a test of the above mechanism an estimate of $2V_{12}$ is available by the present empirical fitting procedure; evidence of the fit to the nd $^1B_1$ data of Dehmer & Holland (1991) are given in table 4. One finds by comparing the bent $\tilde{F}$ nd $^1B_1$ and linear nd $^1B_1$ expansion coefficients in table 1 that the predicted electronic stabilizations of these two states with respect to linear H_2O^+ are 12 070 cm^{-1} and 11 866 cm^{-1}, respectively, giving a difference of 200 cm^{-1} which is remarkably close to the required 190 cm^{-1}. The comparable *ab initio* values are 12 253 cm^{-1} and 12 129 cm^{-1} with a gap of 125 cm^{-1} (Theodorakopoulos *et al.* 1996). The conclusion is that the proposed mechanism gives an excellent estimate of the autoionization rate.

6. Conclusions

An empirical quantum defect synthesis of the known rotationally resolved vibrational states of H_2O and D_2O has been performed and applied to the prediction of perturbations to the bent nd series and to exploration of a possible mechanism of autoionization from the linear nd $^1B_1$ states.

With very few exceptions the quantum defect expansion in equation (2.2) proved remarkably successful in accounting for the vibrational term values of all known bent electronic states. Knowledge of the linear 3p $^1B_2$ state, which is seen as a perturber of the nd series, is limited to bending progressions, but the known levels of H_2O and D_2O could only be reconciled by allowing for a marked reduction in the stretching vibrational frequencies from their H_2O^+ values. A known perturbation to the 3d (000) cluster of H_2O is predicted to be repeated for the 4d (000) $\tilde{E}'$ $^1B_1$ state, but to fall off rapidly for higher nd states. The predicted disposition of bending levels of the linear 3p $^1B_2$ state also rationalizes aspects of the observed rotationally selective predissociation in the $\tilde{E}$ and $\tilde{E}'$ components of the 3d clusters.

A new specifically polyatomic vibronic coupling mechanism for autoionization from the nd $^1B_1$ linear state was shown to account quantitatively for the observed autoionization contribution to the observed linewidth.

Appendix A. New rotational analyses and assignments

Photographic absorption spectra in the region of the 3d (100) $\leftarrow 1b_1$ clusters of H_2O and D_2O, kindly made available by J. W. C. Johns, were analysed by the Coriolis coupled top model of Gilbert *et al.* (1991). The analysis for D_2O, which is quite straightforward, includes the $\tilde{E}$ and $\tilde{F}$ components of the 3d (100) $\leftarrow 1b_1$ cluster and the $4pa_1$ (000) $\leftarrow 1b_1$ band. The $\tilde{E}'$ $^1B_2$ component of the cluster appears only as scattered diffuse lines. On the other hand it proves possible to identify previously unassigned lines in the 3d (000) $\tilde{E}'$ $^1B_2$ band with the $K' = 2$ branches and revised parameters based on the assignment of 29 lines with a standard deviation of 0.5 cm^{-1} are given in table 5.

The situation with respect to H_2O is more complicated. Both Ishiguro *et al.* (1978) and Mayhew (1984) point to a close coincidence between the 3d $\tilde{E}$ (100) $^1B_1$ and 4p (100) $^1B_1$ absorption bands, but only a single band could be identified; it was assigned on the basis of Coriolis anomalies in the upper state A rotational constant to the 4p (100) $^1B_1$ state and the Coriolis coupled fit also led to an approximate origin for the 4p (000) $^1A_1$ state. A second difficulty is that the 3d $\tilde{E}'$ (100) $^1B_2 \leftarrow \tilde{X}$ band contains only $K' = 0$ branches, which points to strong interaction with a predissociated even bending level of the linear 3p $^1B_2$ state. Unpredissociated $K' = 0$ branches of odd v_2' members of this bending progression were reported by Abramson *et al.* (1990); another is responsible for a known perturbation to the $K' = 0$ branches of the 3d (000) $\tilde{E}'$ $^1B_2$ state (Gilbert *et al.* 1991). The final problem is that it has not proved possible to find a convincing simulation for the fully developed $\tilde{F}$ (100) $\leftarrow \tilde{X}$ bands in the absence of knowledge about possible perturbing states; only the $K' = 0$ branch of the $^1B_1 \leftarrow \tilde{X}$ component of this Coriolis mixed $\tilde{F}$ ($^1A_1$, $^1B_1$) band can be identified with complete certainty.

Values of the derived spectroscopic parameters are given in table 5. They are based in the case of the 3d (100) $\tilde{E}$ band of D_2O on 110 assignments with $\sigma = 0.98$ cm^{-1}. The line density in the corresponding $\tilde{F}$ band is much higher and assignments were

1634   *M. S. Child*

Table 5. *Derived spectroscopic parameters*

(Centrifugal constants were taken as those of the positive ion. Values in parenthesis were constrained in the fit.)

state	A (cm^{-1})	B (cm^{-1})	C (cm^{-1})	X (cm^{-1})	quantum defect
H_2O^b					
$\tilde{E}'$ (100) $^1B_2$	[29.06]	9.35±0.25	[9.35]	92 125±2	0.078 12
$\tilde{F}$ (100) $^1B_1$	[29.06]	10.99±0.20	8.97±0.19	92 908±2	−0.015 08
4p (000) $^1B_1$	30.38±0.30	14.03±0.09	8.30±0.04	91 670±1	0.70 334
H_2O^+	29.06^b	12.43^b	8.47^b	101766^c	
D_2O^a					
$\tilde{E}'$ (000) $^1B_2$	12.80±0.17	5.64±0.03	4.32±0.04	89 093±1	
$\tilde{E}$ (100) $^1B_1$	16.47±0.12	6.17±0.07	4.17±0.06	90 998±1	0.123 27
$\tilde{F}$ (100) $^1B_1$	16.23±0.14	6.29±0.12	3.79±0.13	92 198±2	−0.016 46
$\tilde{F}$ (100) $^1A_1$	[16.03]	6.62±0.14	3.90±0.18	92 179±2	−0.014 09
4p (000) $^1B_1$	16.53±0.16	6.32±0.06	4.43±0.03	91 827±1	0.702 03
D_2O^+	16.03^d	6.24^d	4.41^d	101 916^c	

[a]Undetermined origins were taken as follows:

H_2O: $\tilde{D}''$ (100) $^1A_2$ 89 402 cm^{-1}, $\tilde{E}$ (100) $^1B_1$ 91 708 cm^{-1}, 4p (000) $^1A_1$ 92 013 cm^{-1}.
D_2O: $\tilde{D}''$ (100) $^1A_2$ 88 483 cm^{-1}, $\tilde{E}'$ (100) $^1B_2$ 91 440 cm^{-1}, 4p (000) $^1A_1$ 92 134 cm^{-1}.
[b]Lew (1976).
[c]Tonkyn *et al.* (1991).
[d]Lew & Groleau (1987).

restricted to 43 assignments with combination differences less than 0.5 cm^{-1}, or to obvious coincidences between strong experimental and calculated features. These bands contain branches with $K' \leqslant 4$. The corresponding figures for the 4p (000) $^1B_1$ bands are 38 assignments with $\sigma = 1.2$ cm^{-1} for H_2O, 28 assignments with $\sigma = 0.8$ cm^{-1} for D_2O and $K' \leqslant 3$ in both cases. Details of the assignments are available from the author. As discussed above, the vibrational term values X differ from conventional origins ν by omission of rotational terms dependent only on components of the orbital angular momentum ℓ (see Gilbert *et al.* 1991). Quantum defects were determined by assuming ionization energies of 101 766 cm^{-1} for H_2O and 101 916 cm^{-1} for D_2O (Tonkyn *et al.* 1991) and symmetric stretching fundamentals of 3213 cm^{-1} for H_2O^+ (Dinelli *et al.* 1988) and 2342.2 cm^{-1} for D_2O^+ (Reutt *et al.* 1986).

The spectra made available by Johns also include evidence of two new members of the 3p $^1B_2$ linear state bending progression reported by Abramson *et al.* (1990). One is the $v_2' = 5$ band of D_2O according to the latter author's assignment (or $v_2' = 7$ in the scheme adopted in §4), with an origin at 85 991 cm^{-1}. The other is the level responsible for the approximately 100 cm^{-1} perturbation to the $K' = 0$ members of the 3d (000) $\tilde{E}'$ $^1B_2$ state. The perturbed origin of this $v_2' = 7$ level (or $v_2' = 9$, using §4 assignments) lies at 89 205.7 cm^{-1}, while the $J' = K' = 0$ level of $\tilde{E}$ $^1B_2$, which is perturbed by 110.6 cm^{-1} (Gilbert *et al.* 1991) is found at 88 904.6 cm^{-1}. Deperturbation yields an interaction term of 145 cm^{-1} and an unperturbed linear state origin at 89 095 cm^{-1}. The derived spectroscopic parameters are given in table 5.

Phil. Trans. R. Soc. Lond. A (1997)

References

Abramson, E. H., Zhang, J. & Imre, D. G. 1990 *J. Chem. Phys.* **93**, 947.

Ashfold, M. N. R. & Bayley, J. M. 1990 *J. Chem. Soc. Faraday Trans.* **86**, 213.

Ashfold, M. N. R., Bayley, J. M. & Dixon, R. N. 1984*a Can. J. Phys.* **62**, 1806.

Ashfold, M. N. R., Bayley, J. M. & Dixon, R. N. 1984*b J. Chem. Phys.* **84**, 35.

Bell, S. 1965 *J. Mol. Spec.* **16**, 205.

Brommer, M., Weis, B., Follmeg, B., Rosmus, P., Carter, S., Handy, N. C., Werner, H.-J. & Knowles, P. J. 1993 *J. Chem. Phys.* **98**, 5222.

Carter, S., Handy, N. C. & Sutcliffe, B. T. 1983 *Mol. Phys.* **49**, 745.

Child, M. S. & Jungen, Ch. 1990 *J. Chem. Phys.* **93**, 7756.

Connerade, J. P., Baig, M. A., McGlynn, S. P. & Garton, W. R. S. 1980 *J. Phys.* B **13**, L705.

Dehmer, P. M. & Holland, D. M. P. 1991 *J. Chem. Phys.* **94**, 3302.

Dinelli, A. M., Crofton, M. W. & Oka, T. 1988 *J. Mol. Spectrosc.* **127**, 1.

Dixon, R. N. 1985 *Mol. Phys.* **54**, 333.

Dixon, R. N., Duxbury, G., Rabalais, J. W. & Asbrink, L. 1976 *Mol. Phys.* **31**, 423.

Dutuit, O., Tabche-Fouhaile, A., Nenner, I., Frohlich, H. & Guyon, P. M. 1985 *J. Chem. Phys.* **83**, 584.

Gilbert, R. D., Child, M. S. & Johns, J. W. C. 1991 *Mol. Phys.* **74**, 473.

Greene, C. H. & Jungen, Ch. 1985 *Adv. Atom. Mol. Phys.* **21**, 51.

Hirst, D. M. & Child, M. S. 1992 *Mol. Phys.* **77**, 463.

Ishiguro, E., Sasanuma, M., Masuko, H., Moirioka, Y. & Nakamura, M. 1978 *J. Phys.* B **11**, 993.

Lew, H. 1976 *Can. J. Phys.* **54**, 2028.

Lew, H. & Groleau, R. 1987 *Can. J. Phys.* **65**, 739.

Johns, J. W. C. 1963 *Can. J. Phys.* **41**, 209.

Johns, J. W. C. 1971 *Can. J. Phys.* **49**, 944.

Mayhew, C. A. 1984 Ph.D. thesis, Imperial College of Science, Technology and Medicine, London.

Page, R. H., Larkin, R. J., Shen, Y. R. & Lee, Y. T. 1988 *J. Chem. Phys* **88**, 2249.

Petsalakis, I. D., Theodorakopoulos, G. & Child, M. S. 1995 *J. Phys.* B **28**, 5179.

Price, W. C. 1936 *J. Chem. Phys.* **4**, 147.

Reuter, W., Perić, M. & Peyerimhoff, S. D. 1991 *Mol. Phys.* **74**, 569.

Reutt, J. E., Wang, L. S., Lee, Y. T. & Shirley, D. A. 1986 *J. Chem. Phys* **85**, 6928.

Ross, S. C. 1990 *AIP Conf. Proc.* (Caracas, Venezula) **225**, 78.

Smith, P. L., Yoshino, K., Greisinger, H. E. & Black, J. H. 1981 *Astrophys. J.* **250**, 166.

Theodorakopoulos, G., Petsalakis, I. D. & Beunker, R. J. 1985 *J. Chem. Phys.* **96**, 217

Theodorakopoulos, G., Petsalakis, I. D. & Child, M. S. 1996 *J. Phys.* B **29**, 4543.

Theodorakopoulos, G., Nicolaides, C. I., Buenker, R. I. & Peyerimhoff, S. D. 1982 *Chem. Phys. Lett.* **89**, 164.

Theodorakopoulos, G., Nicolaides, C. I., Buenker, R. I. & Peyerimhoff, S. D. 1984 *Chem. Phys. Lett.* **105**, 253.

Tonkyn, R. G., Wiedmann, R., Grant, E. R. & White, M. G. 1991 *J. Chem. Phys.* **94**, 7033.

Vrakking, M. J. J., Lee, Y. T., Gilbert, R. D. & Child, M. S. 1993 *J. Chem. Phys.* **98**, 1902.

Watanabe, K. & Zelikoff, M. 1953 *J. Opt. Soc. Am.* **43**, 753.

Weiss, B., Carter, S., Rosmus, P., Werner, H.-J. & Knowles, P. J. 1989 *J. Chem. Phys.* **91**, 2818.

Discussion

G. Duxbury (*Department of Physics and Applied Physics, University of Glasgow, UK*). In modelling the appearance of $K_a = 0$ vibronic levels in the linear Rydberg states of water, which have the $\tilde{A}\,^2A_1$ of the water as their core, the $\tilde{A}\,^2A_1$ states with $K \leqslant 1$ are assumed to be predissociated via rapid electronic Coriolis (Renner–Teller) coupling to the lower $\tilde{A}\,^2A_1$ electronic state of the ion core states. Since it has been shown that in SiH_2^+, this coupling can be turned off by the generation of a high angular momentum barrier at high values of K_a, is it possible to see fragmentary high K_a systems buried in the Rydberg spectra?

One of the puzzles associated with the studies of the ions of the dihydrides of oxygen, sulphur, selenium and tellurium has been the structure of the photoelectron spectrum corresponding to ionization to the $\tilde{B}\,^2B_2$ electronic state of the ion. The reason for this puzzle is shown in the extensive *ab initio* calculations which Professor Child has recently carried out with Theodorakopoulos and Petsalakis, in which he has confirmed the predictions of other calculations that the $\tilde{B}\,^2B_2$ electronic state of the ion has a very small bond angle. However, none of the high resolution photoelectron spectra of water show the expected long progression in the bending vibration, although attempts have been made to assign some of the irregularities in the pattern to excitation of the bending vibration. The prediction of a small angle state also applies to the other dihydrides for which there is less and less evidence of any bending excitation, and where the progression observed becomes more and more like a progression in the stretching vibration only. Since this peculiar state forms the ion core for some of the Rydberg states of water, is there any explanation for the reasons why the theory and experiment appear to diverge?

M. S. Child. Professor Duxbury's suggestion that the Renner–Teller induced predissociation of the $^1B_2$ linear states could be switched off by angular momentum barriers at sufficiently high K_a is a very interesting one. Any possibility of observing the resulting fragmentary high K_a systems must, however, await a thorough assignment of the higher nd Rydberg clusters.

One part of the answer to Professor Duxbury's question about series terminating on the strongly bent $^2B_2$ state of H_2O^+ is that Reutt *et al.* (1986) do observe bending progressions up to $v_2 = 14$ in the photoelectron bands of H_2O^+ and D_2O^+ at 17–20 eV, which are assigned to $^2B_2$. The bands are, however, very diffuse, with estimated lifetimes of 10–20 fs, due possibly to intersystem crossing to the $^2A_1$ state via a conical intersection (Dehareng *et al.* 1983). The Rydberg spectrum of Ishiguro *et al.* (1978) also contains diffuse bands between 800 and 500 Å which are assigned to $nsa_1 \leftarrow 1b_2$ excitations of H_2O and D_2O. Moreover the *ab initio* studies of Theodorakopoulos *et al.* (1982) indicate direct dissociation from the $3sa_1 \leftarrow 1b_2$ state to produce $O(^1D)+H_2$. The indications are therefore that the $B\,^2B_2$ state of H_2O^+ is strongly dissociative, and that this character is also carried at least to the ns series that terminates on this state.

Additional references

Dehareng, D., Chapuisat, X., Lorquet, J.-C., Galloy, C. & Raseev, G. 1983 *J. Chem. Phys.* **78**, 1246.

Ishiguro, E., Sasanuma, M., Masuko, H., Morioka, Y. & Nakamura, N. 1978 *J. Phys.* B **11**, 993.

Reutt, J. E., Wang, L. S., Lee, Y. T. & Shirley, D. A. 1986 *J. Chem. Phys.* **85**, 6928.

Theodorakopoulos, G., Nicolaides, C. A., Buenker, R. J. & Peyerimhoff, S. D. 1982 *Chem. Phys. Lett.* **89**, 164.